Visible Light Photolysis of Hydrogen Iodide Using Sensitized Layered Metal Oxide Semiconductors: The Role of Surface Chemical Modification in Controlling Back Electron Transfer Reactions

Geoffrey B. Saupe and Thomas E. Mallouk*

Department of Chemistry, The Pennsylvania State University, University Park, Pennsylvania 16802

Won Kim and Russell H. Schmehl

Department of Chemistry, Tulane University, New Orleans, Louisiana 70118

Received: August 16, 1996; In Final Form: December 25, 1996[⊗]

The internally platinized wide bandgap semiconductor $K_4Nb_6O_{17}$ can be sensitized by $[(bpy)_2Ru(4\text{-}(2,2'\text{-bipyrid-4-yl})\text{-phenylphosphonic acid}](PF_6)_2$ (**1**). In aqueous iodide solutions at pH 2, the visible light photolysis of HI, to form H_2 and I_3^-, is catalyzed by **1**/$K_{4-x}H_xNb_6O_{17}$/Pt. The strong bond between the surface and the phosphonate group of **1** allows one to adsorb other surface species, which decrease the rate of the back electron transfer reaction between conduction band electrons and I_3^- ions. Methylphosphonic acid and undecylphosphonic acid do not form good surface monolayers on **1**/$K_{4-x}H_xNb_6O_{17}$ and do not increase the rate of hydrogen evolution. Anionic surface modifiers $[TiNbO_5]_n^{n-}$, derived from exfoliation of $KTiNbO_5$, and poly(styrenesulfonate), PSS, increase the initial hydrogen evolution rate by factors of 3 and 5, respectively. In the latter case, the initial quantum yield for HI photolysis is ca. 3%. Transient diffuse reflectance spectroscopy was used to monitor the formation and disappearance of I_3^- ions with **1**/$K_{4-x}H_xNb_6O_{17}$ and PSS/**1**/$K_{4-x}H_xNb_6O_{17}$. The rate constant for the back electron transfer reaction between conduction band electrons and I_3^- ions decreases from $3.17(\pm0.03) \times 10^7$ to $3.01(\pm0.02) \times 10^6$ M^{-1} s^{-1} upon adsorption of PSS.

Introduction

The sensitization of wide bandgap semiconductor electrodes by visible light absorbing dyes has been a topic of continuing interest since it was first introduced by Gerischer in 1972.[1] This technique, which extends the range of photoactivity of both semiconductor electrodes and semiconductor particles into the wavelength range that is of interest for solar photoconversion applications, has been progressively refined through fundamental studies of dye adsorption and interfacial electron transfer reactions.[2] While early versions of dye-sensitized photoelectrochemical cells were very inefficient,[1] largely because of the low quantum yield of charge injection from the photoexcited dye into the semiconductor, some modern examples have incident photon-to-current conversion efficiencies approaching unity.[3] The impressive quantum and power conversion efficiencies of these dye-sensitized cells, which must have seemed unlikely to early workers in the field, reflect important advances in interfacial design. Sensitizers have been developed that absorb strongly across the spectrum and adsorb to the semiconductor surface in such a way as to promote very rapid photochemical charge injection.[4,5] At the same time, the morphology and interfacial chemistry of semiconductor electrodes has been optimized for improved light absorption and charge separation efficiency.[3]

While dye-sensitized photoelectrochemical cells have become quite efficient, and indeed, because of their low cost, promising for applications in solar-to-electric power conversion, there are no examples of dye-sensitized semiconductor particles that catalyze energy-storing (i.e., nonspontaneous) photochemical reactions efficiently. Despite the chemical similarity of the two systems, there is a vast difference in performance, which arises from two factors. First, in the electrochemical system, a bias can be applied to the photoelectrode that inhibits charge recombination by physically separating (in the case of an n-type semiconductor) injected electrons and oxidized sensitizer and/or donor molecules. Second, in the particle-based system, thermal catalysts are usually required to make chemical products such as hydrogen. These catalysts also accelerate parasitic recombination reactions, which are always spontaneous if free energy is being stored in the desired photochemical process.

Recently, we reported that internally platinized $K_4Nb_6O_{17}$, a lamellar semiconductor, sensitized with RuL_3^{2+} (L = 4,4′-dicarboxy-2,2′-bipyridine) functions as a visible light photocatalyst for the decomposition of aqueous KI solutions to H_2 and I_3^-.[6] Although the quantum efficiency in this system is only 0.3%, it demonstrates an important point, namely that it is possible to make a nonsacrificial hydrogen evolution photocatalyst if care is taken to eliminate (through a molecular sieving effect in this case) the exoergic back reaction between H_2 and the oxidized donor. A subsequent study showed that the poor efficiency of this system is a consequence of the competition between the irreversible conversion of protons and conduction band electrons to molecular hydrogen and the reaction of conduction band electrons with I_3^-.[7] In this paper we demonstrate that it is possible to slow down the latter reaction by adding an anionic polyelectrolyte layer, which repels the oxidized donor from the semiconductor/solution interface. This simple modification increases the initial quantum yield for hydrogen evolution to approximately 3%. While this yield is still very modest compared with that of the best dye-sensitized photoelectrochemical cells, the surface modification strategy may have useful implications for those systems as well.

Experimental Section

Materials. *[(bpy)$_2$Ru(4-(2,2′-bipyrid-4-yl)-phenylphosphonic acid](PF$_6$)$_2$ (**1**).* The ligand diethyl 4-(2,2′-bipyrid-4-yl)phen-

[⊗] Abstract published in *Advance ACS Abstracts,* March 1, 1997.

S1089-5647(96)02531-X CCC: $14.00

ylphosphonate was made by reaction of 4-(*p*-bromophenyl)-2,2′-bipyridine with triethyl phosphite in the presence of tetrakis(triphenylphosphine)palladium(0) with toluene as solvent.[8] The ligand obtained from this reaction was coordinated to Ru(II) by reaction with $Ru(bpy)_2Cl_2$ in ethanol to yield $[(bpy)_2Ru$(diethyl 4-(2,2′-bipyrid-4-yl)phenylphosphonate)$](PF_6)_2$ (elemental analysis for $C_{40}H_{37}N_6O_3P_3F_{12}Ru\cdot H_2O$, found (calcd): C, 44.08 (44.09); H, 3.50 (3.61); N, 7.64 (7.71)). The product obtained in this reaction was hydrolyzed with bromotrimethylsilane in dry acetonitrile to yield the acid $[(bpy)_2Ru$-(4-(2,2′-bipyrid-4-yl)-phenylphosphonic acid$](PF_6)_2$. All other chemicals and solvents used were Aldrich reagent or HPLC grade and were used without further purification. Distilled water was passed through a Barnstead Nanopure II system and had a resistivity of 18 MΩ cm. Aqueous and methanolic solutions were acidified as necessary using 2 M aqueous $HClO_4$.

Photocatalyst Preparation. The proton-exchanged, internally platinized semiconductor $K_{4-x}H_xNb_6O_{17}\cdot nH_2O$ (0.04−0.10 wt % Pt) was prepared as previously described.[7] Surface adsorption of **1** was carried out using an acidic methanol-water solution at pH 2. For every gram of solid, 20 mL of a 50−100 mM solution of **1** was used and the suspension was stirred in the dark for 30 min, then rinsed with pH 2 water or methanol, dried in air, and stored in the dark. The adsorption of **1** is not quantitative under these conditions, and the coverage was determined by difference from the 454 nm absorbance of the supernatant solution. The other surface modifiers (MP, UP, PSS, $[TiNbO_5]_n^{n-}$) were adsorbed subsequent to **1**.

Poly(sodium 4-styrenesulfonate) (PSS) (Aldrich MW 70 000) was adsorbed by stirring 100 mL of a 1 mM solution of PSS at pH 2 with 1 g of sensitized catalyst for 1 h in the dark. After being rinsed with pH 2 water and dried in air, these solids were stored in the dark. The amount of PSS adsorbed was also quantified by means of the absorbance of the supernatant solution. In most cases, only a slight excess of PSS was used, and the solution concentrations before and after adsorption were determined from the 226 nm absorbance of PSS. The performance of the composite improved slightly when a 10-fold excess of PSS was used in the adsorption step, although in this case it was not possible to quantify the coverage accurately by difference.

Undecylphosphonate (UP, Alfa Products) was adsorbed by stirring 0.42 g of sensitized catalyst in 5 mL of methanol and adding 10 μL of a 11.3 mM methanolic solution of UP. Methylphosphonic acid (MP, Aldrich) was adsorbed by stirring 0.65 g of sensitized catalyst in 3 mL of methanol and adding 100 μL of a 1.25 mM methanol solution of MP. The quantity of UP or MP adsorbed was determined by measuring the phosphorus content of the supernatant spectrophotometrically.[9] The phosphonates were converted to orthophosphate by drying the concentrated supernatant solutions on about 20 mg of CaO (Spectrum) followed by ashing over a flame in a Pt boat for 15 s. (Excess CaO caused problems with the precipitation of $CaMoO_4$.) Five drops of concentrated perchloric acid were applied to dissolve the CaO and orthophosphate. In the following order 3 mL of water, 0.5 mL of 20 mM hydrazine in water, and 0.4 mL of sodium molybdate solution (2.5 g of $Na_2MoO_4\cdot H_2O$ in 100 mL of 10 M H_2SO_4) were then added and mixed well. This solution was put in a boiling water bath for 5 min and cooled quickly. Absorbance measurements of the resulting phosphomolybdenum blue in this solution were made at 820 nm using a reagent blank as a reference. Of the 125 nmol of MP reacted with the solid, 14 nmol remained unadsorbed, whereas the 113 nmol of UP was adsorbed quantitatively. UV−visible spectra showed that 25.3 and 65.8 nmol of the sensitizer was desorbed, respectively, in the MP and UP experiments.

$KTiNbO_5$ was stirred in 1 M HCl for 4 days and then filtered and rinsed with water. This procedure was repeated three times in order to ensure complete exchange of H^+ for K^+. Tetrabutylammonium hydroxide (TBA^+OH^-, 40% solution in water, Aldrich) was then added dropwise to a stirred aqueous suspension of the acid-exchanged solid until the pH stablized at 9−10. This procedure produces a colloidal dispersion of $[TiNbO_5]_n^{n-}$ sheets. A solution (5 mL) of this colloid at pH 8 containing ca. 0.50 mg of the TBA^+ salt of $[TiNbO_5]_n^{n-}$ was added to a vigorously stirred suspension of 0.2 g of sensitized catalyst in 3 mL of water. Stirring was continued in the dark for 20 min, and then the solid was filtered, rinsed with pH 2 water, and dried in air. UV−visible spectra showed that 47 nmol of the sensitizer was desorbed during the $TiNbO_5^-$ loading. Analysis of the filtrates and isolated solids gave a $[TiNbO_5]_n^{n-}$ loading of 2 μmol/g.

A triiodide stock solution was prepared by adding solid iodine to pH 2, 100 mM KI to give 0.2 mM I_3^-, which then was diluted as necessary with 100 mM KI, purged with Ar, and kept in the dark before use. Before each photolysis experiment, the concentration of I_3^- was determined from the absorbance at 353 nm, using an extinction coefficient of 26 400 M^{-1} cm^{-1}.[10]

Methods. *Steady State Photolysis.* A 500 W Hg−Xe arc lamp with a 450 ± 50 nm interference filter was focused onto the sample (overall incident power 2.3 mW). To 8.0 mL of water at pH 3 was added 0.11 g of catalyst in a 14 mL quartz vessel, and the solution was purged with Ar for 15 min. A 105 mM KI concentration was created by adding 140 mg of KI to the solution, and a butyl rubber septum was applied. The resulting pH was approximately 2. The head space gas was then purged with Ar for 30 min before photolysis began.

Head space gases were sampled during photolysis by adding 0.40 mL of Ar to the vessel and removing 0.40 mL of gas via an airtight syringe. The gas was injected into a gas chromatograph with a 13X molecular sieve column, held at ambient temperature, and a thermal conductivity detector. The data reported below are corrected for dilution effects caused by sampling.

Instrumentation. Solution UV−vis spectra were collected on a Hewlet-Packard 8452A diode array spectrometer and diffuse reflectance spectra on a Varian DMS-300 equipped with an integrating sphere attachment.

For flash photolysis/transient diffuse reflectance experiments, 1 g of catalyst was mixed with a 100 mM KI solution (pH 2) and purged with Ar in a 1 cm cuvette. A 150 W Xe arc lamp was focused through a shutter window and a 340 nm long pass filter (used to prevent bandgap excitation of the semiconductor) onto the face of the cuvette at 45°. Approximately normal to the Xe light source, a 532 nm, 15 ns pulsed laser (Spectra Physics GCR-13 Nd:YAG, ca. 200 mJ/pulse) illuminated the same area of the cuvette. Diffuse-reflected analyzing light was monitored normal to the cuvette face and focused through a monochromator onto a Hammamatsu photomultiplier tube (PMT) detector biased at 800 V and thermoelectrically cooled to −40 °C. A fast digitizing oscilloscope recorded the PMT output current. Spectra were corrected for the wavelength-dependent penetration depth of the analyzing light in the sample, as described previously.[7]

Because of the relatively long time scale (tens of milliseconds) over which transients were recorded, the data acquisition system used previously[11] was significantly modified. On this time scale, the analyzing light could not be intensified by a lamp pulser, which is typically useful on sub-millisecond time scales.

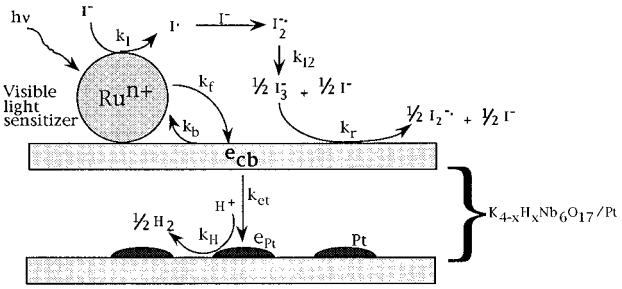

Figure 1. Schematic illustration of the photocatalytic system, showing the components and possible electron transfer pathways.

Increasing the input impedance of the digitizing oscilloscope to 10 kΩ, and cooling the PMT significantly improved the signal to noise ratio in data acquisition while introducing an instrumental time constant of ca. 1 μs. Increasing the sample concentration at the surface of the cuvette had a dramatic effect on signal strength, and the cuvette was therefore filled with suspended solid of sufficient concentration that the powder, which settled slowly, filled the illuminated area. Care was taken to stir and purge the sample with Ar often during the course of the experiments, but not during the actual data acquisition. It was also important to avoid continuous irradiation of the sample with analyzing light between laser shots and to avoid firing the laser too rapidly, as this caused observable particle movement due to heating, expansion, and convection in the sample. Noise (60 Hz) from the laboratory environment, which modulated the analyzing light intensity, was averaged away by collecting multiple shots at each wavelength. Efforts to ground the equipment adequately and to shield the cables and connections were helpful but did not completely eliminate 60 Hz noise.

Results and Discussion

The photocatalytic system we have previously reported is unique as a visible light to chemical energy storage system, in that it uses an electrochemically reversible redox couple as an electron donor.[6,7] In this sense the system resembles a miniaturized, short-circuited version of dye-sensitized photoelectrochemical cells in which the I^-/I_3^- couple is used as the redox shuttle.[3] Photolysis of an aqueous iodide solution in the presence of a sensitized, internally platinized, layered metal oxide semiconductor yields gaseous hydrogen and aqueous I_3^-. Figure 1 shows the idealized structure of this photocatalyst, with the various kinetic pathways available for both the productive forward electron transfer reactions and the nonproductive back reactions. Photoexcited tris(2,2′-bipyridyl-4,4′-dicarboxylate)-ruthenium (RuL_3^{2+}) molecules, adsorbed at the external surface, efficiently transfer electrons to the semiconductor conduction band where they retain sufficient energy to reduce water to molecular hydrogen at the internal platinum sites. The iodide in solution then reduces the resulting RuL_3^{3+} to RuL_3^{2+} and ultimately forms triiodide ions through a complex reaction sequence.

A problem in the system is the back-reaction pathway, represented by the kinetic rate constant k_r, which competes with the forward electron transfer process, represented by k_{et}. Previous studies have shown that minimizing the interlayer distance maximizes k_{et} and results in an improved quantum yield for hydrogen evolution.[7] Attempts to reduce k_r by blocking access of I_3^- to the surface, using, for example, adsorbed surfactants, resulted in desorption of the weakly adsorbed carboxylate sensitizer RuL_3^{2+} and loss of efficiency.

Adsorption of the Sensitizer and Blocking Layers. In the present study, the use of phosphonate sensitizer **1**, which adsorbs much more strongly to the semiconductor surface than analogous carboxylates, allows us to modulate k_r by adsorbing various types of blocking layers at the dye-sensitized semiconductor surface.[12]

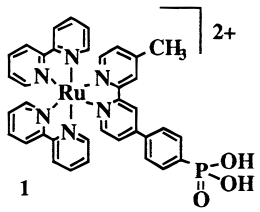

1

Adsorption of **1** onto internally platinized $K_{4-x}H_xNb_6O_{17}\cdot nH_2O$ resulted in a surface loading of 1.43 μmol/g, which is about two times higher than the optimal loading previously found for the carboxylated sensitizer RuL_3^{2+}. Unlike the latter, **1** is freely soluble in the solution from which it is deposited, and hence the adsorption reaction is self-limiting at approximately monolayer coverage. Since the $Ru(bpy)_3^{2+}$ "tail" of **1** has a much larger area than its phenylphosphonate head group, it follows that adsorption of the monolayer leaves free surface sites. Methylphosphonic acid (MP) and undecylphosphonic acid (UP) were chosen as short- and long-chain molecules that could adsorb specifically to these sites. Adsorption of MP and UP onto $\mathbf{1}/K_{4-x}H_xNb_6O_{17}\cdot nH_2O$/Pt gave surface coverages of 0.171 and 0.269 μmol/g, while 0.039 and 0.157 μmol/g of **1** were desorbed, respectively, in the process. Increasing the concentration of MP or UP used and keeping all other conditions the same led to nearly complete desorption of **1** from the solid. This suggests that rather than filling in "holes" in the monolayer of **1**, the alkylphosphonates actually bind by displacing the sensitizer.

Two polymeric blocking layers, poly(styrenesulfonate) (PSS) and $[TiNbO_5]_n^{n-}$, which are presumed to bind via electrostatic interaction with **1**, were also investigated as surface modifiers. Treating the sensitized catalyst with excess aqueous PSS results in a surface coverage of 5.25 μmol/g, which indicates that the PSS layer actually overcompensates the charge of the sensitizer layer. While the sensitizer imparts a positive charge to the unmodified surface, which is probably not altered significantly by the neutral MP and UP adsorbates, it is evident that the excess PSS adsorbed results in a negative surface charge at the pH of the photolysis reaction. In both the PSS and $[TiNbO_5]_n^{n-}$ cases, there was minimal desorption of the sensitizer upon adsorption of the polyanion. This is consistent with an electrostatic binding mechanism, in which PSS or $[TiNbO_5]_n^{n-}$ replaces counterions associated with the adsorbed layer of cationic **1**.

Steady State Photolysis. Steady state data for the visible light photolysis of HI with the unmodified photocatalyst $\mathbf{1}/K_{4-x}H_x$-$Nb_6O_{17}\cdot nH_2O$/Pt and with the same catalyst modified with PSS and $[TiNbO_5]_n^{n-}$ are shown in Figure 2. In all cases the rate of hydrogen evolution is initially constant and becomes progressively slower as the reaction proceeds. The decay in rate does not represent poisoning or irreversible deactivation of the catalyst because the same initial hydrogen evolution rate is obtained when the photolyzed catalyst solution is centrifuged and fresh KI/HI solution is added. The data show that the alkylphosphonate surface modifiers UP and MP have little effect on the rate of hydrogen evolution, whereas $[TiNbO_5]_n^{n-}$ and PSS have a pronounced effect.

The kinetics of the photolysis reaction can be modeled in the steady state approximation by assuming that the concentration of conduction band electrons varies slowly with time, eq 1. This condition is satisfied when the rate represented by the k_f pathway in Figure 1, the charge injection rate, is balanced

$$d[e^-]_{cb}/dt \approx 0 \quad (1)$$

by the sum of the rates from the k_b, k_r, and k_{et} pathways. Using this approximation, one can derive eq 2, in which $[Ru^{2+*}]$ and

$$\frac{d[H_2]}{dt} = \frac{d[I_3^-]}{dt} = \frac{^1/_2 k_f k_{et}[Ru^{2+*}]}{k_b[Ru^{3+}] + k_{et} + k_r[I_3^-]} \quad (2)$$

$[Ru^{3+}]$ represent the concentrations of the excited state and oxidized forms of the sensitizer, respectively. Using an additional steady state approximation (3), for $[Ru^{3+}]$, it is possible to derive the differential rate law (4) in terms of the

$$d[Ru^{3+}]/dt \approx 0 \quad (3)$$

$$\frac{d[I_3^-]}{dt} = \frac{^1/_2 k_f k_{et}[Ru^{2+*}]}{\left(\frac{k_f k_b[Ru^{2+*}]}{[I^-]k_l}\right) + k_{et} + k_r[I_3^-]} \quad (4)$$

photostationary concentration of the excited state of the sensitizer $[Ru^{2+*}]$. This equation can be integrated, using the boundary condition $[I_3^-]_{t=0} = 0$, to give the integrated rate law (5), which expresses $[I_3^-]$ (or equivalently the pressure of hydrogen) as a function of time.

$$[I_3^-] = \frac{1}{k_r}\{-b + \sqrt{b^2 + k_f k_{et} k_r [Ru^{2+*}]t}\} \quad (5)$$

$$\text{where } b \equiv \left(\frac{k_f k_b[Ru^{2+*}]}{[I^-]k_l}\right) + k_{et}$$

Theoretical photolysis curves derived from eq 5 (solid lines) are superimposed on the data shown in Figure 2. The amount of hydrogen evolved increases linearly with time initially and then approximately as the square root of the photolysis time, consistent with the form of eq 5. In all cases, the theoretical curve fits the experimental data early in the reaction but overestimates the rate of HI photolysis after several hours, indicating that the model is an oversimplification at higher I_3^- concentrations. Sampling of the photolyzed solutions verifies that the H_2/I_3^- stoichiometry is close to 1:1 for samples with and without blocking monolayers. For example, an unblocked sample after several hours of photolysis gave 0.43 μmol of H_2 and 0.53 μmol of I_3^-, whereas a PSS-blocked sample gave 1.23 μmol of H_2 and 1.24 μmol of I_3^-.

While the form of hydrogen evolution curves is similar for all samples, there is a striking difference in activity between the unmodified and $[TiNbO_5]_n^{n-}$ and PSS-modified photocatalysts. The activity of the unmodified and alkylphosphonate-modified catalysts are quite similar. This result indicates that electron transfer between the semiconductor surface and I_3^- is not significantly impeded by the presence of MP or UP, either because the alkylphosphonates cover the surface incompletely or because they are not thick enough to block electron transfer. Molecular models show that the MP layer should have a thickness of approximately 5 Å. Such a layer would be too thin to self-assemble in such a way as to exclude solvent molecules or I_3^- ions. The UP molecules, which are approximately 16.4 Å in length in the *all-trans* configuration, would be expected to slow the electron transfer reaction significantly if they form a well-ordered monolayer. Apparently this layer is sufficiently porous to still allow access of I_3^- ions to the surface. It should be noted, by analogy to alkanethiolate

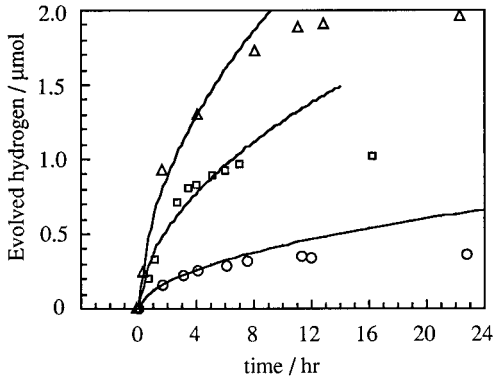

Figure 2. Hydrogen evolution from the steady photolysis of $K_{4-x}H_x$-Nb_6O_{17}/Pt sensitized with **1** and modified with PSS (triangles) and $[TiNbO_5]_n^{n-}$ (squares) and unmodified (circles).

monolayers on gold, that UP may be of insufficient length to form a well-ordered self-assembled monolayer at room temperature.[13] UP also lacks polar tail groups, which are beneficial in forming well-ordered monolayers of shorter-chain surfactant molecules.[14]

The adsorption of $[TiNbO_5]_n^{n-}$ or PSS has a pronounced effect on the photolysis reaction, resulting in a 3- to 5-fold increase in the initial hydrogen evolution rate. In the case of PSS the initial rate corresponds to a quantum yield, per incident photon, of 3%. We postulate that the effect of the added polyanion layer is to exclude I_3^- and $I_2^{-\bullet}$ from the catalyst surface, thereby greatly reducing k_r. This hypothesis is supported by the direct measurement of k_r, using time-resolved spectroscopic techniques.

Flash Photolysis Experiments. From eq 5 it is evident that k_r, the rate constant for charge recombination of e_{cb} and I_3^-, cannot be extracted from the hydrogen evolution curves without knowledge of k_f, k_{et}, and $[Ru^{2+*}]$. Transient spectroscopic measurements provide a more direct and quantitative measure of charge-recombination rates for the unmodified and PSS-modified samples. Photoexcitation of the sensitized composite leads to rapid charge transfer from **1** to the semiconductor via reactions 6 and 7. Charge recombination can occur through

$$Ru^{2+} \xrightarrow{h\nu} Ru^{2+*} \quad (6)$$

$$Ru^{2+*} \xrightarrow{k_f} Ru^{3+} + e^-_{cb} \quad (7)$$

reaction 8 or can be intercepted by reaction 9, which regenerates the ground state Ru^{2+} form of the sensitizer. Iodine radicals formed in reaction 9 quickly combine with I^- to form $I_2^{-\bullet}$, which decays to the product I_3^- through second-order reaction 10. Under the high light intensity conditions of flash photolysis, reaction 10 occurs on a time scale of microseconds.[7]

$$Ru^{3+} + e^-_{cb} \xrightarrow{k_b} Ru^{2+} \quad (8)$$

$$Ru^{3+} + I^- \xrightarrow{k_l} Ru^{2+} + I^\bullet \xrightarrow[I^-]{\text{fast}} Ru^{2+} + I_2^{-\bullet} \quad (9)$$

$$2I_2^{-\bullet} \xrightarrow{k_{I_2}} I_3^- + I^- \quad (10)$$

Figure 3 shows transient difference spectra acquired 500 μs after the laser flash, which show the expected I_3^- peak in the ultraviolet. Transient spectra for samples with and without PSS show maxima at 380 and 360 nm, respectively. The latter is close to the expected absorbance maximum for I_3^- in aqueous solution at 353 nm.[10] The red shift in the I_3^- absorbance band

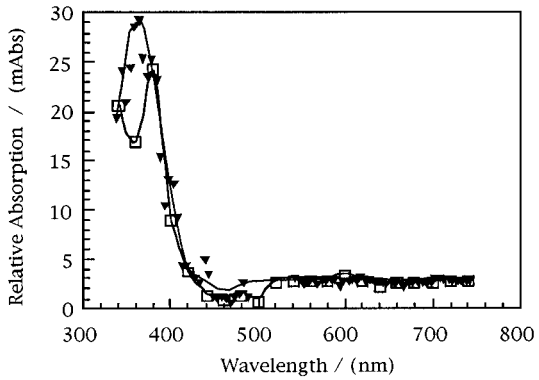

Figure 3. Transient diffuse reflectance spectra of unmodified **1**/$K_{4-x}H_x$-Nb_6O_{17} (triangles) and a PSS-modified sample (squares) acquired 500 μs after 532 nm excitation. Zero milliabsorbance units corresponds to base line diffuse reflectance measured prior to the 10 ns laser flash.

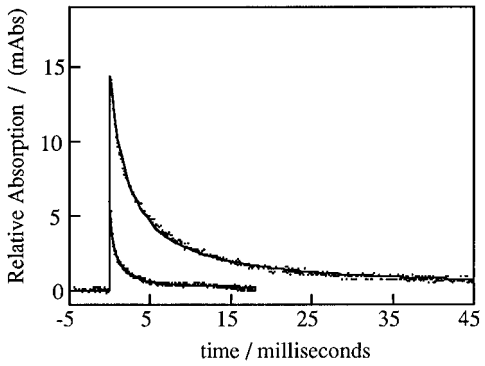

Figure 4. Average of 20 transient diffuse reflectance traces, acquired at 380 nm, for an unmodified sample and for a sample modified with PSS, showing the difference in time scales for the charge-recombination reaction of e_{cb} and I_3^-. Second-order fits (solid lines) are superimposed on the data points.

in the case of the PSS sample suggests that the presence of PSS changes the electronic environment of the I_3^- ion at the surface.

Charge recombination, which is the ultimate fate of conduction band electrons in the absence of interlayer Pt, occurs in the model presented in Figure 1 via reaction 11. Transient

$$I_3^- + e^-_{cb} \xrightarrow{k_r} I_2^{-\bullet} + I^- \qquad (11)$$

decays that reflect this kinetic process are shown for unmodified and for PSS-modified samples in Figure 4. The difference in the two decays reflects a large difference in k_r for the two samples. Good second-order fits to the decays were obtained, which gave rate constants of $3.17(\pm 0.03) \times 10^7$ and $3.01(\pm 0.02) \times 10^6$ M^{-1} s^{-1}, respectively, for the two samples. While the actual values of these rate constants depend on an assumption about the path length of the analyzing light,[15] the ratio of rate constants (approximately 10) does not and is in qualitative agreement with the enhanced hydrogen evolution rate found in the presence of PSS. Interestingly, the relative absorbance value at time zero is significantly enhanced by the presence of PSS. This indicates that the effect of PSS is not simply the inhibition of charge recombination (11) of $e^-_{(cb)}$ with solution-phase I_3^- ions. PSS is either reducing the local concentration of I_3^- by displacing surface-adsorbed anions or modulating the rate of the back reaction 8 as well.

Effect of Added I_3^-. The kinetic model represented by eqs 2−4 predicts that the reaction rate, at appreciable I_3^- concentrations, should vary as $[I_3^-]^{-1}$. In order to test this model, samples were deliberately spiked with known concentrations of I_3^-, and

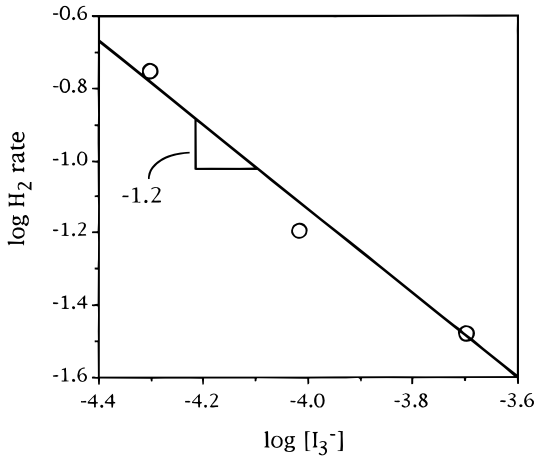

Figure 5. Plot of log(initial rate) vs log $[I_3^-]$ for PSS-modified samples.

the initial rate of hydrogen evolution was monitored under steady state photolysis conditions. Figure 5 shows plots of log(initial rate) vs log($[I_3^-]$) for the PSS-modified samples. The slope of the line shows that the initial rate varies as $[I_3^-]^{-1.2}$, i.e., that there is a stronger dependence on $[I_3^-]$ than predicted by the simple steady state model. We postulate that the deficiency in the model arises from an oversimplification of the back electron transfer reaction 11. A second back-reaction pathway that is coupled to the first, represented by reaction 12, also exists

$$I_2^{-\bullet} + e^-_{cb} \xrightarrow{k_{r2}} 2I^- \qquad (12)$$

$I_2^{-\bullet}$ is generated in reactions 9 and 11 and consumed in reactions 10 and 12, and the system thus becomes quite complex kinetically. Reduction of I_3^- at the semiconductor surface, reaction 11, generates $I_2^{-\bullet}$, which consumes another electron via reaction 12. This is consistent with the observed dependence of initial rate on $[I_3^-]$, which suggests that more than one electron is consumed per I_3^- ion. Since $I_2^{-\bullet}$ is generated at the particle surface and decays via both interfacial and homogeneous reactions, its concentration is spatially inhomogeneous. The concentration of I_3^- is likewise inhomogeneous, since it is coupled to $I_2^{-\bullet}$ through reactions 10 and 11. The problem therefore becomes a rather intricate one involving diffusion and convection, in addition to the interfacial and homogeneous electron transfer reactions. Attempts to arrive at an analytical solution that reproduces the observed dependence of rate on $[I_3^-]$ have been unsuccessful because of the complexity of the system.

Conclusions

The efficiency of HI photolysis catalyzed by sensitized $K_{4-x}H_xNb_6O_{17}{\cdot}nH_2O$/Pt is controlled by the competition between interlayer forward electron transfer, which results in the irreversible production of molecular hydrogen, and back electron transfer at the semiconductor−solution interface. The phosphonate sensitizer **1** adsorbs sufficiently strongly to the surface of $K_{4-x}H_xNb_6O_{17}{\cdot}nH_2O$ that it is possible to add other adsorbed species, which modulate the rate of the back electron transfer reactions between the semiconductor and oxidized donor anions I_3^- and $I_2^{-\bullet}$. Simple alkylphosphonates MP and UP do not form sufficiently compact monolayers to affect the rate of the back electron transfer reaction at low concentration, and displace the sensitizer at high concentration. However, polyanions $[TiNbO_5]_n^{n-}$ and PSS have a marked effect on this rate, which is reflected both in steady state photolysis and transient absorbance measurements. These results may have interesting consequences for other systems, such as sensitized semiconduc-

tor photoelectrochemical cells, where back electron transfer reactions are to be avoided. The successful derivitization of one semiconductor, $K_{4-x}H_xNb_6O_{17}\cdot nH_2O$, with monolayers of a different one, $[TiNbO_5]_n^{n-}$, also suggests interesting possibilities for the preparation of more complex semiconductor heterostructures derived from layered transition metal oxides. The properties of these heterostructures are currently under investigation in this laboratory.

Acknowledgment. This work was supported by the Division of Chemical Sciences, Office of Basic Energy Sciences, Department of Energy, under contract DE-FG02-93ER14374. We thank Drs. Timothy Rhodes and Stephen Atherton and Prof. Wayne Jones for help with the design of instrumentation and software used in transient spectroscopic experiments. This paper is dedicated to the memory of Heinz Gerischer.

References and Notes

(1) (a) Gerischer, H. *Photochem. Photobiol.* **1972**, *16*, 243.

(2) (a) Spitler, M. T.; Calvin, M. *J. Chem. Phys.* **1977**, *66*, 4294. (b) Gleria, M.; Memming, R. *Z. Phys. Chem., Neue Folge* **1975**, *98*, 302. (c) Clark, W. D. K. *J. Am. Chem. Soc.* **1977**, *99*, 4676. (d) Memming, R.; Schröppel, F.; Bringmann, U. *J. Electroanal. Chem.* **1979**, *100*, 307. (e) Hamnett, A.; Dare-Edwards, M. P.; Wright, R. D.; Seddon, K. R.; Goodenough, J. B. *J. Phys. Chem.* **1979**, *83*, 3280. (f) Dare-Edwards, M. P.; Goodenough, J. B.; Hamnett, A.; Seddon, K. R.; Wright, R. D. *Faraday Discuss. Chem. Soc.* **1980**, *70*, 285. (g) Frei, H.; Fitzmaurice, D. J.; Grätzel, M. *Langmuir* **1990**, *6*, 198. (h) Kamat, P. V. *Chem. Rev.* **1993**, *93*, 267.

(3) (a) O'Regan, B.; Grätzel, M. *Nature* **1991**, *353*, 737. (b) Nazeeruddin, M. K.; Kay, A.; Rodicio, I.; Humphry-Baker, R.; Müller, E.; Liska, P.; Vlachopoulos, N.; Grätzel, M. *J. Am. Chem. Soc.* **1993**, *115*, 6382. (c) Pechy, P.; Rotzinger, F. P.; Nazeeruddin, M. K.; Kohle, O.; Zakeeruddin, S. M.; Humphry-Baker, R.; Grätzel, M. *J. Chem. Soc., Chem. Commun.* **1995**, 65. (d) Hagfeldt, A.; Grätzel, M. *Chem. Rev.* **1995**, *95*, 49.

(4) (a) Desilvestro, J.; Grätzel, M.; Kavan, L.; Moser, J. *J. Am. Chem. Soc.* **1985**, *107*, 2988. (b) Liska, P.; Vlachopoulos, N.; Nazeeruddin, M. K.; Comte, P.; Grätzel, M. *J. Am. Chem. Soc.* **1988**, *110*, 3686. (c) Amadelli, R.; Argazzi, R.; Bignozzi, C. A.; Scandola, F. *J. Am. Chem. Soc.* **1990**, *112*, 7099. (d) Argazzi, R.; Bignozzi, C. A.; Heimer, T. A.; Castellano, F. N.; Meyer, G. J. *Inorg. Chem.* **1994**, *33*, 5741. (e) Argazzi, R.; Bignozzi, C. A.; Heimer, T. A.; Castellano, F. N.; Meyer, G. J. *J. Am. Chem. Soc.* **1995**, *117*, 11815.

(5) (a) Spitler, M. T.; Parkinson, B. A. *Langmuir* **1986**, *2*, 549. (b) Chau, L.-K.; Osburn, E. J.; Armstrong, N. R.; O'Brien, D. F.; Parkinson, B. A. *Langmuir* **1994**, *10*, 351.

(6) Kim, Y. I.; Salim, S.; Huq, M. J.; Mallouk, T. E. *J. Am. Chem. Soc.* **1991**, *113*, 9561.

(7) Kim, Y. I.; Atherton, S. J.; Brigham, E. S.; Mallouk, T. E. *J. Phys. Chem.* **1993**, *97*, 11802.

(8) Full details of the synthesis of **1** will be reported elsewhere: Kim, W. Y.; Liang, Y.; Schmehl, R. H., manuscript in preparation.

(9) Marczenko, Z. *Separation and Spectrophotometric Determination of Elements*; Ellis Horwood: New York, 1986; p 447.

(10) Awtrey, A. D.; Connick, R. E. *J. Am. Chem. Soc.* **1951**, *73*, 1842.

(11) Keller, S. W.; Johnson, S.; Saupe, G. B.; Yonemoto, E. H.; Brigham, E. S.; Mallouk, T. E. *ACS Symp. Ser.*, in press.

(12) For related studies involving surface-adsorbed phosphonate monolayers and sensitizers, see ref 3c and the following. (a) Yan, S. G.; Hupp, J. T. *J. Phys. Chem.* **1996**, *100*, 6867. (b) Folkers, J. P.; Gorman, C. B.; Laibinis, P. E.; Buchholz, S.; Whitesides, G. M.; Nuzzo, R. G. *Langmuir* **1995**, *11*, 813.

(13) Porter, M. D.; Bright, T. B.; Allara, D. L.; Chidsey. C. E. D. *J. Am. Chem. Soc.* **1987**, *109*, 3559.

(14) Miller, C.; Cuendet, P.; Gratzel, M. *J. Phys. Chem.* **1991**, *95*, 877.

(15) In order to extract the second-order charge-recombination rate constant from transient diffuse reflectance data, the effective path length of the analyzing light in the sample had to be determined. This was accomplished by using an aqueous solution of $Ru(bpy)_3^{2+}$ and methylviologen dichloride, for which the charge-recombination rate constant is known, in the presence of alumina (on which neither component adsorbs) as a scatterer. An effective path length of 0.11 mm was calculated for 380 nm analyzing light. Full details are given in ref 11.